



AAS 98-168

Station-Keeping Strategies for Translunar Libration Point Orbits

G. Gómez
Departament de Matemàtica
Aplicada i Anàlisi
Universitat de Barcelona
Barcelona, Spain

K. Howell
School of Aeronautics and
Astronautics
Purdue University
West Lafayette, Indiana

J. Masdemont
Departament de Matemàtica
Aplicada I
Universitat Politècnica
de Catalunya
Barcelona, Spain

C. Simó
Departament de Matemàtica
Aplicada i Anàlisi
Universitat de Barcelona
Barcelona, Spain

AAS/AIAA Space Flight Mechanics Meeting

Monterey, California

9-11 February 1998

AAS Publications Office, P.O. Box 28130, San Diego, CA 92128

STATION-KEEPING STRATEGIES FOR TRANSLUNAR LIBRATION POINT ORBITS

G. Gómez,^{*} K. Howell,[†] J. Masdemont,[‡] C. Simó[§]

Spacecraft in orbits near the collinear libration points are proving to be excellent platforms for scientific investigations of various phenomena. Since such libration point trajectories are generally unstable, spacecraft moving on such paths must use some form of trajectory control to remain close to their nominal orbit. The primary goal of this effort is the study of two particular station-keeping approaches applied to the maintenance of a spacecraft in an quasiperiodic Earth-Moon L_2 halo orbit. The Target Point strategy and the Floquet Mode approach both use maneuvers executed (impulsively) at discrete time intervals. The analysis includes some investigations of a number of the problem parameters that affect the overall cost. Preliminary results are summarized.

INTRODUCTION

As part of the trajectory design, some current missions and a number of recent proposals have included halo or Lissajous orbits in the vicinity of the L_1 or L_2 libration points, most notably in the Sun-Earth/Moon barycenter system. This effort is directed toward comparison and further development of two particular station-keeping approaches that can be used to maintain spacecraft near such libration point trajectories. Each type of analysis offers unique insights into the problem that may be mutually beneficial. In this case, the investigation is conducted in the quicker Earth-Moon system; the reference orbit is a halo orbit computed in a full solar system model.

Halo and Lissajous orbits are solutions that represent bounded motion in the vicinity of a collinear libration point. The problem of controlling a spacecraft moving near an inherently unstable libration point orbit is of current interest. In the late 1960's, Farquhar¹ suggested several station-keeping strategies for nearly-periodic solutions near the collinear points. Later, in 1974, a station-keeping method for spacecraft moving on halo orbits in the vicinity of the Earth-Moon translunar libration point (L_2) was published

^{*} Departament de Matemàtica Aplicada I Anàlisi, Universitat de Barcelona, Gran Via 585, 08007 Barcelona, Spain.

[†] School of Aeronautics and Astronautics, 1282 Grissom, Purdue University, West Lafayette, Indiana, USA 47907.

[‡] Departament de Matemàtica Aplicada I, Universitat Politècnica de Catalunya, E.T.S.E.I.B., Diagonal 647, 08028 Barcelona, Spain.

[§] Departament de Matemàtica Aplicada I Anàlisi, Universitat de Barcelona, Gran Via 585, 08007 Barcelona, Spain.

by Breakwell, Kamel, and Ratner.² These studies assumed that the control could be modelled as continuous. In contrast, specific mission requirements influenced the station-keeping strategy for the first libration point mission. Launched in 1978, the International Sun-Earth Explorer-3 (ISEE-3) spacecraft remained in a near-halo orbit associated with the interior libration point (L_1) of the Sun-Earth/Moon barycenter system for approximately three and one half years.³ Impulsive maneuvers at discrete time intervals (up to 90 days) were successfully implemented as a means of trajectory control. Since that time, more detailed investigations have resulted in various station-keeping strategies, including the two identified here as the Target Point and Floquet Mode approaches.

The Target Point method (as presented by Howell and Pernicka,⁴ Howell and Gordon,⁵ and Keeter⁶) computes corrective maneuvers by minimizing a weighted cost function. The cost function is defined in terms of a corrective maneuver as well as position and velocity deviations from a nominal orbit at a number of specified future times t_i . The nominal state vectors at each time t_i are denoted as "target points." The target points are selected along the trajectory at discrete time intervals that are downstream of the maneuver. In contrast, the Floquet Mode approach, as developed by Simó, Gómez, Llibre, and Martinez,⁷⁻⁸ incorporates invariant manifold theory and Floquet modes to compute the maneuvers. Floquet modes associated with the monodromy matrix are used to determine the unstable component corresponding to the local error vector. The maneuver is then computed such that it eradicates the dominant unstable component of the error. It is noted that both approaches have been demonstrated in a complex model, but neither of these methods has previously been applied in the Earth-Moon system.

THE MODEL AND THE NOMINAL ORBIT

This investigation is directed towards a preliminary evaluation of the Target Point and Floquet Mode station-keeping strategies applied in the Earth-Moon system. Insight from this study should aid future efforts to explore combinations of strategies that might best support a libration point mission.

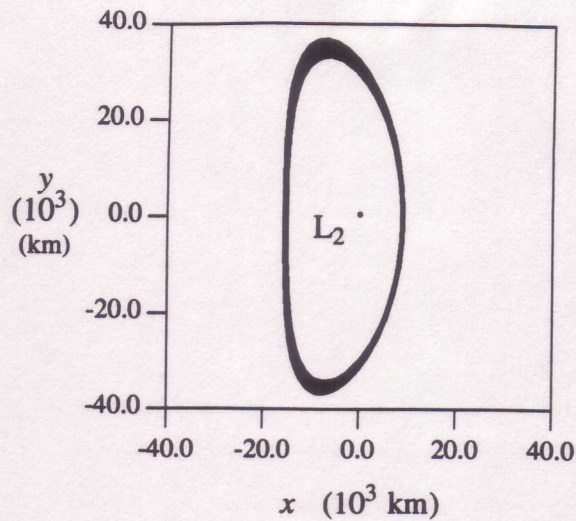
The dynamical model adopted to represent the forces on the spacecraft includes the gravitational influences of the Sun, Moon, and all nine planets using the JPL DE403 ephemeris. Although solar radiation pressure is not currently in the model, the simulation algorithms are general in nature and can be expanded later to incorporate solar radiation pressure (and/or other perturbing forces). The nominal orbit is a quasiperiodic trajectory in the vicinity of the L_2 libration point as defined in the Earth-Moon system. A critical component in the performance of any station-keeping strategy is a good nominal orbit. In the present case, this means a trajectory with little residual acceleration in the dynamical system as modeled by DE403. This is accomplished using an iterative procedure, that is, multiple shooting, which matches the orbit intervals, starting from an initial guess.⁹

Computation of nominal orbits around the collinear libration points of the Sun-Earth system, starting from an initial guess computed in the restricted three-body problem

presents no problems. However, in the case of the Earth-Moon system, strong difficulties appear and the procedure fails when the orbit spans more than two years. The cause is the solar perturbation that results in an initial guess that is far from the real solution. To overcome this difficulty, the initial guess is obtained from a quasi-bicircular model, which is a simplified model where the Earth, Moon and Sun move in almost circular orbits around the Earth-Moon barycenter.¹⁰ The difference between the quasi-bicircular and the bicircular model is that in the latter, all the orbits of the massive bodies are circular and so the movement of the Earth, Moon and Sun is not a true solution of the three-body problem. The movement of the Earth, Moon and Sun in the quasi-bicircular model is computed to be near circular but coherent, that is, a solution of the general three-body problem. Thus, the difference between the former models is essential in the sense that the quasi-bicircular is closer to the real Earth-Moon-Sun system and produces good initial guesses for the multiple shooting procedure, while the simpler bicircular does not.

Starting with the halo orbits computed in the quasi-bicircular model, the multiple shooting procedure⁹ is used for computing trajectories extending for more than 19 years (approximately the Saros period when the Earth, Moon and Sun have almost the same relative positions), meaning that halo orbits for longer time spans can be obtained. The output of the multiple shooting process consists of an orbit split into subintervals and including jump discontinuities in positions and velocities at the matching points, usually spaced one day apart. The jump discontinuities are less than 1 mm in position and less than 1 mm/day in velocities, much smaller than the tracking errors. For practical purposes, the nominal orbit can be considered as a continuous trajectory.

The plot in Figure 1 includes three orthographic projections of the nominal trajectory used in this investigation. Although computations are done in cartesian coordinates, it is desirable to display trajectories in terms of coordinates corresponding to the usual rotating frame with origin at L_2 . The three axes associated with the figure are then defined consistent with the rotating frame typically used in the restricted three-body problem. Thus, the x axis is directed from the larger primary (Earth) to the smaller (Moon), the y axis is defined in the plane of the orbit of the primaries and 90° from the x axis, and the z axis completes the right handed frame. The orbit is plotted relative to L_2 , but the dynamical L_2 libration point does not actually exist in this Earth-Moon system in the same sense that it does in the restricted problem since the motion of the primaries is not actually precisely periodic and includes the gravity fields of the Sun and other planets (the locations of which are all determined using ephemerides). Figure 1 is accomplished by using the known location of L_2 in the restricted problem to compute a corresponding approximate geometric libration point in the system defined by the "full" model. These geometric L_i points retain some properties of the original points in the restricted problem. Thus, the near-halo orbit in the figure still exists. Note that the trajectory is classified as a "southern" orbit. A total of approximately 50 revolutions, over 737 days, appear in the figure. The maximum out-of-plane excursion in the z direction is approximately 16,600 km below a mean lunar orbit plane.



L₂ Southern Class Halo Orbit
Earth-Moon System
 Approximate $A_z=16,600$ km
 Approximate $A_y=37,000$ km
 24 June 2002 to 1 July 2004

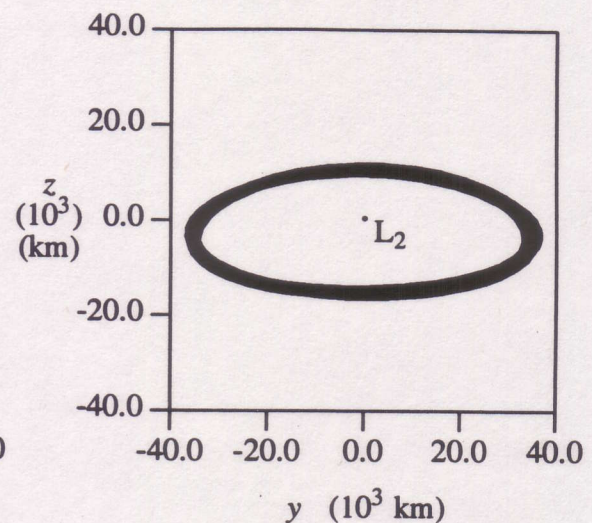
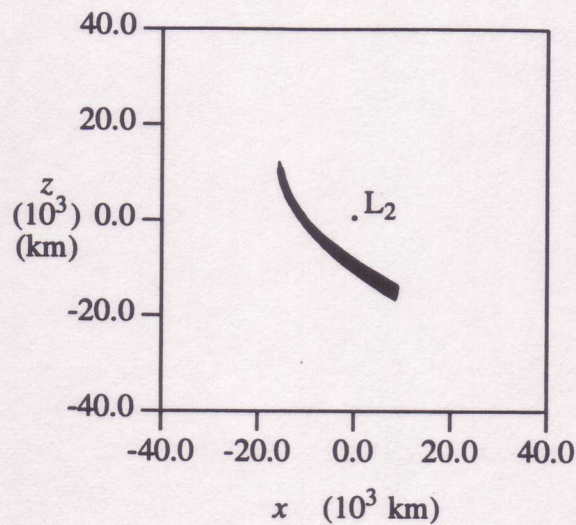


Figure 1 Nominal Halo Orbit in the Earth-Moon System

For both station-keeping strategies discussed here, the nominal orbit and its state transition matrix (STM) must be available at any time along the orbit in a computationally convenient manner. Inaccurate representations contribute to higher maneuver costs. The nominal orbit is computed as a set of discrete points. However, the Target Point algorithm requires the states at arbitrary times. In this case, therefore, the orbit is stored using a spline technique. For the spline data points, a frequency of .15 days yields errors much less than the tracking errors for a trajectory in the Earth-Moon system of 2500 days duration. Unfortunately, the size of the data files precludes this approach as a convenient method to store the 36 elements of the state transition matrix. Rather than attempt to represent each element, the simulation software will reproduce the state transition matrix associated with the nominal orbit, as needed, by numerically integrating the variational equations assuming motion of the gravitational bodies consistent with the model. It is noted that this approach depends heavily on an accurate representation of the nominal orbit.

STATION-KEEPING STRATEGIES

Once the nominal orbit is specified, strategies must be implemented to keep the actual spacecraft trajectory sufficiently close to the nominal path. All maneuvers are assumed to be impulsive and occur at discrete times.

Target Point Approach

The goal of the Target Point station-keeping algorithm is to compute and implement maneuvers to maintain a spacecraft "close" to the nominal orbit, i.e., within a region that is locally approximated in terms of some specified radius centered about the reference path. To accomplish this task, a control procedure is derived from minimization of a cost function. The cost function, J , is defined by weighting both the control energy required to implement a station-keeping maneuver, $\Delta \mathbf{v}$, and a series of predicted deviations of the six-dimensional state from the nominal orbit at specified future times. The cost function includes several submatrices from the state transition matrix. For notational ease, the state transition matrix is partitioned into four 3×3 submatrices as

$$\Phi(t_k, t_o) = \begin{bmatrix} A_{ko} & B_{ko} \\ C_{ko} & D_{ko} \end{bmatrix}. \quad (1)$$

The controller, in this formulation, computes a $\Delta \mathbf{v}$ in order to change the deviation of the spacecraft from the nominal path at some set of future times. The cost function to be minimized is written in general as

$$J = \Delta \mathbf{v}^T Q \Delta \mathbf{v} + \mathbf{p}_1^T R \mathbf{p}_1 + \mathbf{v}_1^T R_v \mathbf{v}_1 + \mathbf{p}_2^T S \mathbf{p}_2 + \mathbf{v}_2^T S_v \mathbf{v}_2 + \mathbf{p}_3^T T \mathbf{p}_3 + \mathbf{v}_3^T T_v \mathbf{v}_3, \quad (2)$$

where superscript T denotes transpose. The variables in the cost function include the corrective maneuver, $\Delta \mathbf{v}$ at some time t_c , and \mathbf{p}_1 , \mathbf{p}_2 , and \mathbf{p}_3 that are defined as 3×1 column vectors representing linear approximations of the expected deviations of the actual spacecraft trajectory from the nominal path (if no corrective action is taken) at specified future times t_1 , t_2 , and t_3 , respectively. Likewise, the 3×1 vectors \mathbf{v}_1 , \mathbf{v}_2 , and \mathbf{v}_3 represent deviations of the spacecraft velocity at the corresponding t_i . The future times at which predictions of the position and velocity state of the vehicle are compared to the nominal path are denoted as target points. They are represented as Δt_i such that $t_i = t_o + \Delta t_i$. The choice of identifying *three* future target points is arbitrary.

In Eqn. (2), Q , R , S , T , R_v , S_v , and T_v are 3×3 weighting matrices. The weighting matrix Q is symmetric positive definite; the other weighting matrices are positive semi-definite. The weighting matrices are generally treated as constants that must be specified as inputs. Selection of appropriate weighting matrix elements is a trial and error process that has proven to be time-consuming. A methodology has been developed that automatically selects and updates the weighting matrices for each maneuver. This "time-varying" weighting matrix algorithm is based solely on empirical observations.

Determination of the $\Delta \mathbf{v}$ corresponding to the relative minimum of this cost function allows a linear equation for the optimal control input, i.e.,

$$\begin{aligned} \Delta \mathbf{v}^* = & - \left[Q + B_{10}^T R B_{10} + B_{20}^T S B_{20} + B_{30}^T T B_{30} + D_{10}^T R_v D_{10} + D_{20}^T S_v D_{20} + D_{30}^T T_v D_{30} \right]^{-1} \\ & \times [(B_{10}^T R B_{10} + B_{20}^T S B_{20} + B_{30}^T T B_{30} + D_{10}^T R_v D_{10} + D_{20}^T S_v D_{20} + D_{30}^T T_v D_{30}) \mathbf{v}_o \\ & + (B_{10}^T R A_{10} + B_{20}^T S A_{20} + B_{30}^T T A_{30} + D_{10}^T R_v C_{10} + D_{20}^T S_v C_{20} + D_{30}^T T_v C_{30}) \mathbf{p}_o], \quad (3) \end{aligned}$$

where \mathbf{v}_o is the residual velocity (3×1 vector) and \mathbf{p}_o is the residual position (3×1 vector) relative to the nominal path at the time t_o . The performance of the modified Target Point algorithm is not yet truly "optimal," though it has been demonstrated to successfully control the spacecraft at reasonable costs. This accomplishment alone provides the user with a quick and efficient way to obtain reasonable station-keeping results. Given some procedure to select the weighting matrices, the maneuver is computed from Eqn. (3). The corrective maneuver ($\Delta \mathbf{v}^*$) is a function of spacecraft drift (in both position and velocity with respect to the nominal orbit), the state transition matrix elements associated with the nominal orbit, and the weighting matrices. It is assumed here that there is no delay in implementation of the maneuver; the corrective maneuver occurs at the time t_o , defined as the current time. Note that this general method could certainly accommodate inclusion of additional target points. Although the nominal orbit that is under consideration here is quasiperiodic, the methodology does not rely on periodicity; it should be applicable to any type of motion in this regime.

In this application, three additional constraints are specified in the station-keeping procedure to restrict maneuver implementation. First, the time elapsed between successive maneuvers must be greater than or equal to a specified minimum time interval, t_{min} . This constraint may be regulated by the orbit determination process, scientific payload requirements, and/or mission operations. Time intervals of one to three days are considered in the Earth-Moon system. The second constraint is a scalar distance (p_{min}) and specifies a minimum deviation from the nominal path (an isochronous correspondence) that must be exceeded prior to maneuver execution. For distances less than p_{min} , maneuver computations do not occur. Third, in the station-keeping simulation, the magnitude of position deviations are compared between successive tracking intervals. If the magnitude is *decreasing*, a maneuver is not calculated. For a corrective maneuver to be computed, all three criteria must be satisfied simultaneously.

After a maneuver is calculated by the algorithm, an additional constraint is specified on the minimum allowable maneuver magnitude, Δv_{min} . If the magnitude of the calculated $\Delta \mathbf{v}$ is less than Δv_{min} , then the recommended maneuver is cancelled. This constraint is useful in avoiding "small" maneuvers that are approximately the same order of magnitude as the maneuver errors. It also serves to model actual hardware limitations.

Floquet Mode Approach

An alternate strategy for station-keeping is the Floquet Mode approach, a method that is significantly different from the Target Point approach. It can be easily formulated in the circular restricted three-body problem. In this context, the nominal halo orbit is periodic. The variational equations for motion in the vicinity of the nominal trajectory are linear with periodic coefficients. Thus, in general, both qualitative and quantitative information can be obtained about the behavior of the nonlinear system from the monodromy matrix, M , which is defined as the state transition matrix (STM) after one revolution along the full halo orbit.

The knowledge of the dynamics of the flow around a halo orbit, or any solution close to it, allows other possibilities than the station-keeping procedure described here, such as the computation of transfer orbits both between halo orbits and from the Earth to a halo orbit.^{11,12} The behavior of the solutions in a neighborhood of the halo orbits is determined by the eigenvalues, λ_i , $i=1,\dots,6$ and eigenvectors \mathbf{e}_i , $i=1,\dots,6$ of M . Gathering the eigenvalues by pairs, their geometrical meaning is the following:

- a) The first pair (λ_1, λ_2) , with $\lambda_1 \cdot \lambda_2 = 1$ and $\lambda_1 \approx 1500$, is associated with the unstable character of the small and medium size halo orbits. The eigenvector, $\mathbf{e}_1(t_o)$, associated with the largest eigenvalue, λ_1 , defines the most expanding direction, related to the unstable nature of the halo orbit. The image under the variational flow of the initial vector $\mathbf{e}_1(t_o)$, together with the vector tangent to the orbit, defines the linear approximation of the unstable manifold of the orbit. In a similar way, $\mathbf{e}_2(t_o)$ can be used to compute the linear approximation of the stable manifold.
- b) The second pair $(\lambda_3, \lambda_4) = (1, 1)$ is associated with neutral variables (i.e., non-unstable modes). However, there is only one eigenvector with eigenvalue equal to one. This vector, $\mathbf{e}_3(t_o)$, is the tangent vector to the orbit. The other eigenvalue, $\lambda_4 = 1$, is associated with variations of the energy (or the period) of the orbit through the family of halo orbits. Along the orbit, the vectors \mathbf{e}_3 and \mathbf{e}_4 span an invariant plane under the flow. The monodromy matrix restricted to this plane has a Jordan form

$$\begin{pmatrix} 1 & \varepsilon \\ 0 & 1 \end{pmatrix}.$$

The value of ε is non zero due to the variations of the period along the family.

- c) The third couple, (λ_5, λ_6) , is formed by two complex conjugated eigenvectors of modulus one. The restriction of the flow to the corresponding two-dimensional invariant subspace, is essentially a rotation. This behavior is related to the existence of quasiperiodic halo orbits around the halo orbit.⁹

When considering dynamical models of motion different from the restricted three-body problem, halo orbits are no longer periodic, and the monodromy matrix is not defined. Nevertheless, for quasiperiodic motions close to the halo orbit (and also for the

Lissajous orbits around the equilibrium point) the unstable and stable manifolds subsist. The neutral behavior can be slightly modified including some instability which, from a practical point of view, is negligible when compared with the one associated with λ_1 .

Instead of the vectors $e_i(t)$ it is convenient to use the Floquet modes $\bar{e}_i(t)$ which, for the periodic case, are defined as six periodic vectors from which the $e_i(t)$ can be easily recovered.¹³ For instance $\bar{e}_1(t)$ is defined as $e_1(t) \cdot \exp[-(t/T) \ln \lambda_1]$, where T is the period of the halo orbit. The control algorithm is developed to utilize this information for station-keeping purposes. The emphasis is placed on formulating a controller that will effectively eliminate the unstable component of the error vector, $\delta(t) = (\delta x, \delta y, \delta z, \delta \dot{x}, \delta \dot{y}, \delta \dot{z})$, defined as the difference between the actual coordinates obtained by tracking and the nominal ones computed isochronously on the reference orbit. At any epoch, t , δ can be expressed in terms of the Floquet modes

$$\delta(t) = \sum_{i=1}^6 \alpha_i \bar{e}_i(t). \quad (4)$$

The controller objective is to add a maneuver such that the magnitude of the component of the error vector in the unstable direction, α_1 , is reduced to zero. The five remaining components do not produce large departures from the reference orbit. By contrast, the component of the error vector along the unstable mode increases by a factor of λ_1 in each revolution.

Denoting the impulsive maneuver as $\Delta = (0, 0, 0, \Delta_x, \Delta_y, \Delta_z)^T$, to cancel the unitary unstable Floquet mode, requires

$$\frac{\bar{e}_1}{\|\bar{e}_1\|} + (0, 0, 0, \Delta_x, \Delta_y, \Delta_z)^T = \sum_{i=2}^6 c_i \bar{e}_i(t). \quad (5)$$

From these equations $\Delta_x, \Delta_y, \Delta_z$ can be obtained as a function of c_5 and c_6 . These free parameters are determined by either imposing a constraint on the available directions of the control or by minimizing a suitable norm of Δ .

For practical implementation it is useful to compute the so-called projection factor along the unstable direction. It is defined as the vector π such that $\delta \cdot \pi = \alpha_1$. Note that for the computation of π only the Floquet modes are required, so it can be computed and stored together with the nominal orbit. To annihilate the unstable projection, α_1 , with a maneuver, $\Delta v = (0, 0, 0, \Delta_x, \Delta_y, \Delta_z)^T$ we ask $(\delta + \Delta v) \cdot \pi = 0$. In this way,

$$\Delta_x \pi_4 + \Delta_y \pi_5 + \Delta_z \pi_6 + \alpha_1 = 0, \quad (6)$$

is obtained, where π_4, π_5 , and π_6 are the last three components of π . Choosing a two axis controller, with $\Delta_z = 0$, and minimizing the Euclidean norm of Δv , the following expressions for Δ_x and Δ_y are obtained,

$$\Delta_x = -\frac{\alpha_1 \pi_4}{\pi_4^2 + \pi_5^2}, \quad \Delta_y = -\frac{\alpha_1 \pi_5}{\pi_4^2 + \pi_5^2}. \quad (7)$$

In a similar way, a one or three axis controller can be formulated.

Once the magnitude of the maneuver is known, an important consideration is the determination of the epoch at which it must be applied. The study of this question requires the introduction of the gain function, $g(t) = \|\Delta\|^{-1}$, where Δ is the unitary impulsive maneuver. It measures the efficiency of the control maneuver along the orbit to cancel the unitary unstable component. This component is obtained using the projection factors and the error vector. As the projection factor changes along the orbit, the same error vector has different unstable components. It is natural then to consider a maneuver delay until reaching another epoch with a better gain. Of course, the gain can increase but the unstable component also increases. So, the function to be studied is

$$R(t) = \frac{\exp\left(t \ln\left(\frac{\lambda_1}{T}\right)\right)}{g(t)}. \quad (8)$$

However, as seen in Figure 2,⁷ this function is always increasing, therefore, it is never good to wait for a maneuver except for operational reasons.

Similar to the Target Point approach, several constraints that impact the maneuvers are specified in the procedure. Some of the most relevant are the time interval between two consecutive tracking epochs (tracking interval), the minimum time interval

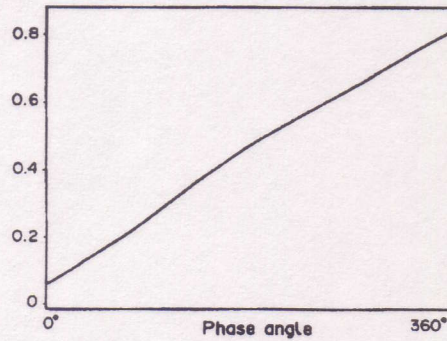


Figure 2 Typical behavior of the function $R(t)$ along a full revolution of a halo orbit. The orbit is parameterized by a phase angle varying between 0 and 360 degrees.

between maneuvers, and the minimum value of α_1 that can not be considered due solely to tracking errors.

Special emphasis must be placed on the evolution of α_1 . With no tracking errors, the evolution of this parameter is exponential with time. When adding tracking errors, and in order to prevent a useless maneuver, this value must be greater than the minimum. So, the minimum value must be selected as a function of the orbit determination accuracy. On the other hand, the value of α_1 should not be too large because this increases the value of the maneuver in an exponential way. Thus, a maximum value is chosen such that if α_1 is greater than the maximum, a control maneuver will be executed to cancel the unstable component. When α_1 is between minimum and maximum values, the error can be due to small oscillations around the nominal orbit. In this case, a maneuver is executed only if the error has been growing at an exponential rate in the previous time steps and the time span since the last maneuver agrees with the one selected. Also, as in the case of the Target Point approach, if the magnitude of the calculated Δv is less than Δv_{min} , then the recommended maneuver is cancelled. In contrast with the Target Point approach, once these parameters have been fixed, there are no more free variables allowing any further minimization.

SOME RESULTS

The impact of a number of the quantifiable parameters on total mission cost has been considered in this investigation in conjunction with the effort to evaluate the Target Point and Floquet Mode station-keeping strategies. The final step in preparing both algorithms for evaluation is determination of input values for a "baseline case." For the Target Point method using constant weighting matrices, the inputs are first selected with the sole purpose of successfully controlling the spacecraft without regard to maneuver costs. Then, the inputs are adjusted (by trial and error) to reduce the total cost. When a set of input values produces an acceptable "minimum" cost, the set is specified as the "baseline" case. Parameters of interest can then be varied independently to investigate the impact on the performance of the station-keeping approach relative to the baseline case. For the Floquet Mode approach, and assuming that the tracking interval, the time interval between consecutive maneuvers, and the minimum magnitude of a maneuver have been fixed, the remaining baseline parameters are estimated from the knowledge of the behavior of the variational equations and the values of the tracking errors. With this data, the minimum and maximum values of the unstable component and the rate of escape from the nominal orbit are estimated. Related to these data there is another parameter, namely the number of consecutive tracking points selected in order to establish if the real trajectory has an exponential escape or not. The value of this integer parameter is related to the rate of escape and the time intervals specified for tracking and execution of maneuvers.

Target Point Results

Values corresponding to the baseline inputs selected for the Target Point station-keeping strategy appear in Table 1. All three target points are used to compute the cost, and predicted errors at each target point are considered. (Since, without solar radiation pressure in the model, the magnitudes of the velocity residuals are much less than the position residuals,⁵ no velocity deviations are considered at this time., i.e., ($R_v = S_v = T_v = 0$)). Standard deviations for the error models are selected to correspond to those published in other works when available. All weighting matrices are diagonal. Units on elements of the weighting matrices are selected to be consistent with velocity values in m/s and position values in km.

Using these inputs and this operational structure in the Target Point station-keeping algorithm, Monte Carlo simulations based on 100 trials are undertaken and baseline results are produced. Consider an example such that the minimum time between maneuvers is 2 days; the tracking interval is 12 hours. In this case, it is assumed that $\Delta v_{min} = 0$. To present output in the appropriate format, tabulated values corresponding to quantities useful in representing the vehicle maneuver history during the simulated mission are stored for each trial. To obtain data that is more representative of the station-keeping performance, the results from 100 trials are averaged. Statistics corresponding to

TABLE 1 Baseline Inputs for Target Point Approach

| Inputs | Baseline Value |
|--|---|
| Orbit Injection Date | June 24, 2002 |
| Trajectory Duration | 737 days |
| Tracking and orbit injection errors: $\sigma_x, \sigma_y, \sigma_z$ $\sigma_{\dot{x}}, \sigma_{\dot{y}}, \sigma_{\dot{z}}$ | 1.0 km, 1.0 km, 1.0 km 1.0 cm/s, 1.0 cm/s, 1.0 cm/s |
| Maneuver errors: $\sigma_{\Delta_x}, \sigma_{\Delta_y}, \sigma_{\Delta_z}$ | 5 %, 5 %, 2 % |
| Min Time Between Maneuvers: Track Int | 1 day : 3 h, 6 h, 12 h, 24 h 2 days: 3 h, 6 h, 12 h, 24 h, 48 h 3 days: 6 h, 12 h, 24 h, 48 h, 72 h |
| Target points weighted in position | 3 |
| Target points weighted in velocity | 0 |
| $\Delta t_1, \Delta t_2, \Delta t_3$ (baseline case) | 3.0, 5.0, 7.0 days |
| Q (nondimensional) (baseline case) | $diag[3.9 \times 10^{11} \quad 3.9 \times 10^{11} \quad 3.9 \times 10^{11}]$ |
| R ($1/s^2$) (baseline case) | $diag[1.0 \times 10^1 \quad 1.0 \times 10^1 \quad 1.0 \times 10^1]$ |
| S ($1/s^2$) (baseline case) | $diag[1.0 \times 10^0 \quad 1.0 \times 10^0 \quad 1.0 \times 10^0]$ |
| T ($1/s^2$) (baseline case) | $diag[1.0 \times 10^{-1} \quad 1.0 \times 10^{-1} \quad 1.0 \times 10^{-1}]$ |

the total cost and total number of maneuvers associated with the baseline case are listed below where Δv_{tot} is the total Δv cost per year and n_{man}/yr is the average number of maneuvers over one year.

| | |
|-------------------------------------|--------------------------|
| Δv_{tot} : Ave = 504.6 cm/s | n_{man}/yr : Ave = 136 |
| Range: Ave = 469.5cm/s – 543.9 cm/s | Pos Dev: Ave = 27.35 km |
| Min Δv : Ave = 2.0 cm/s | |
| Max Δv : Ave = 17.8 cm/s | |

Beyond the example, a number of other cases are simulated and appear in Table 2. Three parameters that influence the performance of the Target Point algorithm are investigated: t_{min} , Δv_{min} , and target point placement. The summary in the table includes all simulations assuming $\Delta v_{min} = 2$ cm/s. Three different values of t_{min} (minimum time allowed between maneuvers) are represented. Also, column 2 lists the average values of total cost per sample, along with the range; average values of the minimum Δv in each sample is listed in column 3; average maximum Δv values appear in column 4; column 5 lists the average number of maneuvers (n_{man}) per year over the samples; and, finally, the average maximum position deviation just prior to a maneuver is listed in the last column. It is notable that in the case corresponding to the baseline, the only difference between the baseline and the result seen in the table is the value of the minimum magnitude of a maneuver (Δv_{min}) that is implemented. In Table 2, the value has increased from zero to 2 cm/s. The higher value corresponds to a lower cost since the maneuvers are no longer trying to correct simply the noise in the tracking data. Table 3 shows the same cases repeated for $\Delta v_{min} = 3$ cm/s.

In general, the results indicate that the algorithm can hold onto the vehicle throughout the duration of the simulation. (The weighting matrices are selected to produce reasonable results but have not necessarily been optimized.) The cost increases as the time interval between maneuvers reaches 3 days. For a given t_{min} , the cost also increases for longer tracking intervals. This is tied tightly to the spacecraft drift at the time of the maneuver and argues for watching the drift carefully. However, in the long term, once a pattern is established, the constant weighting matrices can, in fact, maintain control over the 737 days. Figure 3 includes data from one sample simulation; a trial was arbitrarily selected from the sample seen in Table 2 for $t_{min} = 2$ days and a tracking interval of 12 hours. Over the length of the simulation, the position deviation just prior to the maneuver is plotted as a function of time. A linear approximation to the data also appears. Note that the slope is not positive. This trend also appeared for an orbit of 2500 days in duration. Finally, seen in Figure 4(a), is a plot of the $x - y$ projection of the orbit in which all the maneuvers have been indicated by an open circle. Observe that, with a minimum time between maneuvers of 2 days and an orbit for which one revolution requires approximately 14.4 days, the maneuvers are distributed around the orbit. In Figure 4(b), the four largest maneuvers – all greater than 9.5 cm/s – are indicated.

TABLE 2 Results: Target Point Strategy (Constant Weighting Matrices)

$$\Delta v_{\min} = 2 \text{ cm/s}$$

| Input Parameters | Δv_{tot} (cm/s/yr) | | Min Δv (cm/s) | Max Δv (cm/s) | n_{man}/yr | Max Dev (km) |
|-----------------------------|--------------------------------------|-----------------|--------------------------|--------------------------|----------------------------|-----------------|
| | Ave | Range | Ave | Ave | Ave | Ave |
| $t_{\min} = 1 \text{ day}$ | | | | | | |
| track int: 3 hrs | 323.3 | 308.2 – 343.0 | 2.003 | 4.557 | 132 | 8.902 |
| 6 hrs | 350.6 | 334.4 – 363.1 | 2.002 | 5.427 | 132 | 10.770 |
| 12 hrs | 386.1 | 368.3 – 410.8 | 2.003 | 7.562 | 127 | 12.368 |
| 24 hrs | 509.9 | 467.5 – 548.3 | 2.006 | 13.284 | 120 | 14.142 |
| $t_{\min} = 2 \text{ days}$ | | | | | | |
| track int: 3 hrs | 457.7 | 412.7 – 489.7 | 2.006 | 10.537 | 133 | 25.054 |
| 6 hrs | 485.7 | 434.5 – 526.2 | 2.009 | 11.579 | 124 | 25.986 |
| 12 hrs | 490.8 | 431.6 – 549.3 | 2.016 | 18.282 | 105 | 31.667 |
| 24 hrs | 559.5 | 492.4 – 587.4 | 2.022 | 17.171 | 106 | 18.304 |
| 48 hrs | 1152.2 | 944.2 – 1467.5 | 2.093 | 99.668 | 80 | 79.757 |
| $t_{\min} = 3 \text{ days}$ | | | | | | |
| track int: 3 hrs | 584.6 | 531.1 – 638.1 | 2.014 | 18.581 | 108 | 37.086 |
| 6 hrs | 629.3 | 577.1 – 674.7 | 2.020 | 21.965 | 105 | 25.775 |
| 12 hrs | 643.1 | 596.6 – 695.2 | 2.041 | 23.001 | 98 | 25.114 |
| 24 hrs | 724.6 | 672.6 – 828.8 | 2.068 | 28.118 | 88 | 28.132 |
| 48 hrs | 1185.6 | 1059.4 – 1360.5 | 2.446 | 64.992 | 81 | 55.481 |

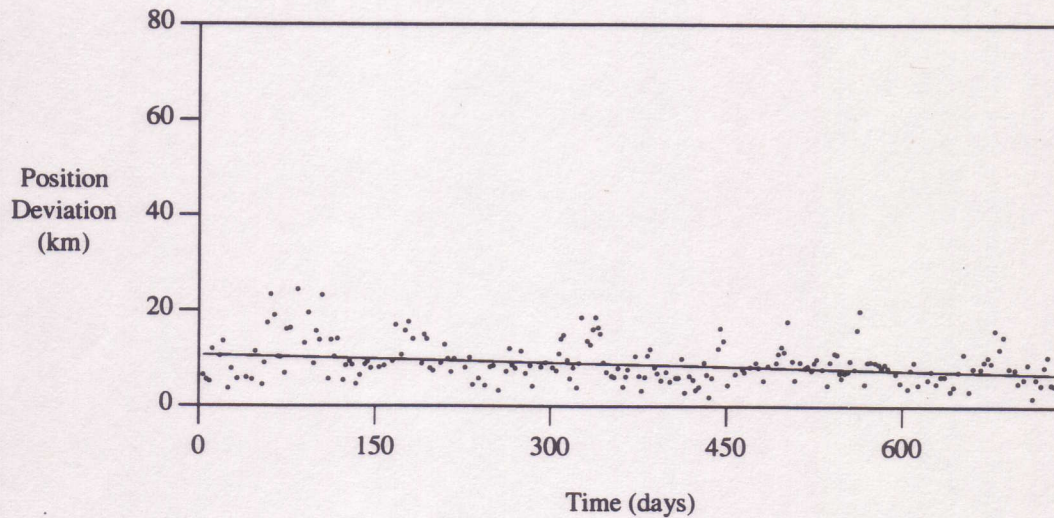


Figure 3 Sample: Position Deviation just Prior to Maneuver

TABLE 3 Results: Target Point Strategy (Constant Weighting Matrices)

$$\Delta v_{min} = 3 \text{ cm/s}$$

| | Δv_{tot} (cm/s/yr) | | Min Δv (cm/s) | Max Δv (cm/s) | n_{man}/yr | Max Dev (km) |
|--------------------------|-------------------------------|----------------|--------------------------|--------------------------|--------------|-----------------|
| Input Parameters | Ave | Range | Ave | Ave | Ave | Ave |
| $t_{min} : 1 \text{ da}$ | | | | | | |
| track int: 3 hrs | 448.8 | 416.0 – 470.4 | 3.001 | 5.395 | 129 | 12.282 |
| 6 hrs | 421.0 | 400.0 – 434.8 | 3.004 | 6.449 | 114 | 13.688 |
| 12 hrs | 494.2 | 450.6 – 552.3 | 3.014 | 10.176 | 116 | 15.563 |
| 24 hrs | 526.0 | 491.8 – 575.1 | 3.018 | 13.694 | 99 | 14.969 |
| $t_{min} : 2 \text{ da}$ | | | | | | |
| track int: 3 hrs | 428.9 | 382.7 – 480.2 | 3.003 | 10.274 | 104 | 26.391 |
| 6 hrs | 470.0 | 423.6 – 517.7 | 3.008 | 11.955 | 101 | 28.877 |
| 12 hrs | 503.2 | 455.1 – 562.2 | 3.006 | 18.076 | 93 | 30.376 |
| 24 hrs | 581.7 | 516.3 – 658.7 | 3.019 | 18.510 | 94 | 20.231 |
| 48 hrs | 1028.8 | 952.3 – 1144.3 | 3.093 | 56.456 | 77 | 49.342 |
| $t_{min} : 3 \text{ da}$ | | | | | | |
| track int: 3 hrs | 584.3 | 545.2 – 635.3 | 3.013 | 20.798 | 97 | 43.029 |
| 6 hrs | 618.1 | 568.3 – 659.4 | 3.009 | 20.461 | 96 | 24.008 |
| 12 hrs | 644.8 | 604.5 – 718.4 | 3.039 | 26.202 | 89 | 30.242 |
| 24 hrs | 734.4 | 652.3 – 842.5 | 3.047 | 31.604 | 84 | 28.946 |
| 48 hrs | 1112.4 | 902.9 – 1352.6 | 3.180 | 62.617 | 79 | 49.970 |

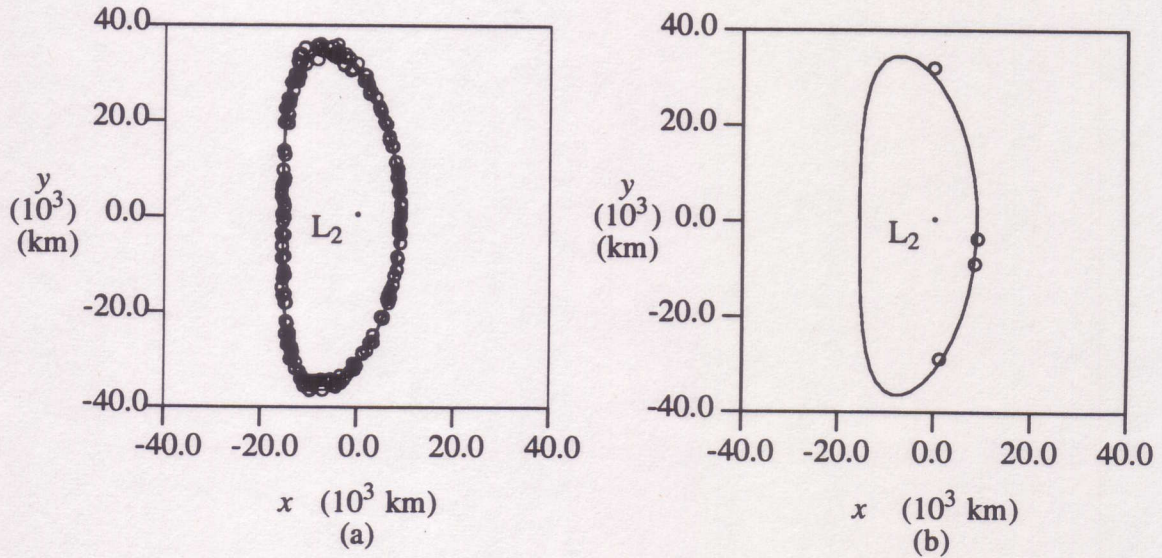


Figure 4 Locations for Sample Case: (a) All Maneuvers (b) Maneuvers > 9.5 cm/s

Floquet Mode Results

Using the input parameters given in Table 4, 100 trials of Monte Carlo simulations have been done. The statistics appear in Tables 5 and 6.

If the errors in tracking and execution of maneuvers are zero, the total cost of the station-keeping should be zero but it is not. This is due to the propagation of the round-off errors during the integration and the highly unstable character of the nominal orbit. The results for this situation give some insight of how the procedure behaves. In Figure 4 (top) the evolution of the unstable component is shown. Each discontinuity corresponds to a maneuver. As it is clearly seen, after each maneuver, the unstable component is "almost" annihilated. Then it starts growing in an exponential way until a maximum value is reached, and then a control is applied. When the maneuver is applied with some error in its execution, the unstable component is not canceled "exactly" and the departure from the nominal is faster.

The sample of results given in Tables 5 and 6 show different facts. The first one is that the best results are obtained when using time intervals for the execution of maneuvers, t_{min} , of one or two days. If this time interval is increased, controllability can be lost, in the sense that, at some moment, the algorithm may be forced to execute very large maneuvers. This is seen by looking at the value of the averaged maximum

TABLE 4 Baseline Inputs for Floquet Mode Approach

| Inputs | Values |
|---|--|
| Orbit Injection Date: | June 24, 2002 |
| Trajectory Duration: | 737 Days |
| Tracking and orbit injection errors: | |
| $\sigma_x, \sigma_y, \sigma_z$ | 1.0 km, 1.0 km, 1.0 km |
| $\sigma_{\dot{x}}, \sigma_{\dot{y}}, \sigma_{\dot{z}}$ | 1.0 cm/s, 1.0 cm/s, 1.0 cm/s |
| Maneuver errors: | |
| $\sigma_{\Delta_x}, \sigma_{\Delta_y}, \sigma_{\Delta_z}$ | 5%, 5%, 2% |
| Min Time Between Man: Track Int | 1 day: 3 h, 6 h, 12 h, 24 h 2 days: 3 h, 6 h, 12 h, 24 h, 48 h 3 days: 6 h, 12 h, 24 h, 48 h, 72 h |
| No. of Points to Detect Escape: | 2, 3, 4, 6 |
| Base of Exponential Escape: | 1.55 |
| Minimum Unstable Component: | 2×10^{-10} |
| Maximum Unstable Component: | 4×10^{-10} |
| Δv_{min} | 2, 3, 5 cm/s |

TABLE 5 Results: Floquet Mode Strategy; $\Delta v_{\min} = 2$ cm/s;
3 points to detect exponential escape

| | Δv_{tot} (cm/s/yr) | | Min Δv (cm/s) | Max Δv (cm/s) | n_{man}/yr |
|---------------------|--------------------------------------|------------------|--------------------------|--------------------------|----------------------------|
| Input Parameters | Ave | Range | Ave | Ave | Ave |
| $t_{\min} : 1$ da | | | | | |
| Track int: 3 hrs | 728.83 | 633.90 – 812.20 | 1.89 | 9.09 | 195 |
| 6 hrs | 641.80 | 554.00 – 734.60 | 1.98 | 9.64 | 147 |
| 12 hrs | 577.66 | 491.40 – 654.50 | 2.19 | 9.52 | 116 |
| 24 hrs | 552.41 | 479.10 – 750.30 | 2.96 | 12.15 | 96 |
| $t_{\min} : 2$ da | | | | | |
| Track int: 3 hrs | 629.90 | 577.30 – 691.70 | 1.92 | 14.35 | 143 |
| 6 hrs | 566.86 | 506.60 – 642.90 | 1.97 | 14.14 | 121 |
| 12 hrs | 550.85 | 482.50 – 617.90 | 2.21 | 13.94 | 103 |
| 24 hrs | 545.02 | 463.90 – 672.10 | 2.99 | 14.63 | 90 |
| 48 hrs | 621.19 | 517.20 – 1100.90 | 3.41 | 21.83 | 82 |
| $t_{\min} : 3$ da | | | | | |
| Track int: 6 hrs | 626.02 | 534.90 – 1004.30 | 2.01 | 28.28 | 100 |
| 12 hrs | 597.69 | 501.50 – 1014.00 | 2.19 | 26.12 | 91 |
| 24 hrs | 596.25 | 514.00 – 846.90 | 2.99 | 25.98 | 84 |
| 48 hrs | 745.20 | 620.10 – 1146.20 | 3.50 | 41.99 | 71 |
| 72 hrs | 747.83 | 630.20 – 1132.70 | 3.46 | 40.11 | 74 |

maneuver performed. For $t_{\min} = 1$ day, a maximum value of 12.15 cm/s is obtained; for $t_{\min} = 2$ days, this value increases to 21.83 cm/s and for three days, it is 41.99 cm/s. These values are almost independent of the rest of the available parameters that remain free. Once t_{\min} is fixed, and the tracking time interval is varied, the best results are always obtained for values of the tracking interval between 12 hours and 1 day (depending on the value of t_{\min}). This is also true if we vary the minimum magnitude of Δv_{\min} and/or the number of sample points used to detect exponential escape. Even if we select $\Delta v_{\min} = 2$ cm/s, in many simulations this value is too low. A minimum value of $\Delta v_{\min} = 4$ cm/s (of this order) seems to be a suitable one. Even the values between two consecutive maneuvers, which are not given in the table, for the parameters of Table 5 with $t_{\min} = 2$ days and a tracking interval of 12 hours, the time between maneuvers ranges between 2 days (which is the minimum one selected) and 14 days which is almost one revolution.

TABLE 6 Results: Floquet Mode Strategy; $\Delta v_{\min} = 2$ cm/s;
3 points to detect exponential escape

| | Δv_{tot} (cm/s/yr) | | Min Δv (cm/s) | Max Δv (cm/s) | n_{man}/yr |
|---------------------|-------------------------------|------------------|--------------------------|--------------------------|--------------|
| Input Parameters | Ave | Range | Ave | Ave | Ave |
| $t_{\min} : 1$ da | | | | | |
| Track int: 3 hrs | 804.00 | 753.40 – 881.50 | 2.74 | 9.04 | 191 |
| 6 hrs | 674.21 | 600.00 – 761.90 | 2.81 | 9.17 | 147 |
| 12 hrs | 583.20 | 522.10 – 764.40 | 2.97 | 9.86 | 115 |
| 24 hrs | 552.00 | 479.10 – 770.70 | 3.19 | 12.36 | 95 |
| $t_{\min} : 2$ da | | | | | |
| Track int: 3 hrs | 667.37 | 599.50 – 759.10 | 2.79 | 14.73 | 136 |
| 6 hrs | 594.42 | 501.40 – 679.50 | 2.82 | 13.63 | 119 |
| 12 hrs | 556.05 | 490.70 – 693.80 | 2.96 | 14.02 | 102 |
| 24 hrs | 545.63 | 463.80 – 751.00 | 3.21 | 15.35 | 90 |
| 48 hrs | 621.19 | 517.20 – 1100.90 | 3.41 | 21.83 | 82 |
| $t_{\min} : 3$ da | | | | | |
| Track int: 6 hrs | 635.41 | 558.00 – 941.80 | 2.87 | 27.07 | 98 |
| 12 hrs | 601.06 | 485.90 – 849.80 | 2.99 | 26.73 | 90 |
| 24 hrs | 601.81 | 515.00 – 1081.40 | 3.25 | 26.79 | 84 |
| 48 hrs | 745.49 | 620.10 – 1146.20 | 3.51 | 42.01 | 71 |
| 72 hrs | 747.83 | 630.20 – 1132.70 | 3.46 | 40.11 | 74 |

Concluding Remarks

This preliminary investigation involves implementation and analysis of two station-keeping strategies for spacecraft moving on a quasiperiodic orbit in the vicinity of the translunar libration point in the Earth-Moon system. Several areas of concern are highlighted and potential ideas for improvement are suggested. Of note is the fact that both approaches can maintain control of the vehicle over the duration of the simulation. Although the Target Point approach is more straightforward, a clear advantage in favor of the Floquet Mode approach is the qualitative information and analysis that becomes available. This may be more critical in the faster Earth-Moon system. In any case, some combination of these ideas is likely to improve the results. The simplicity and robustness and robustness of the Target Point method can complement the qualitative advantages of the Floquet Mode approach.

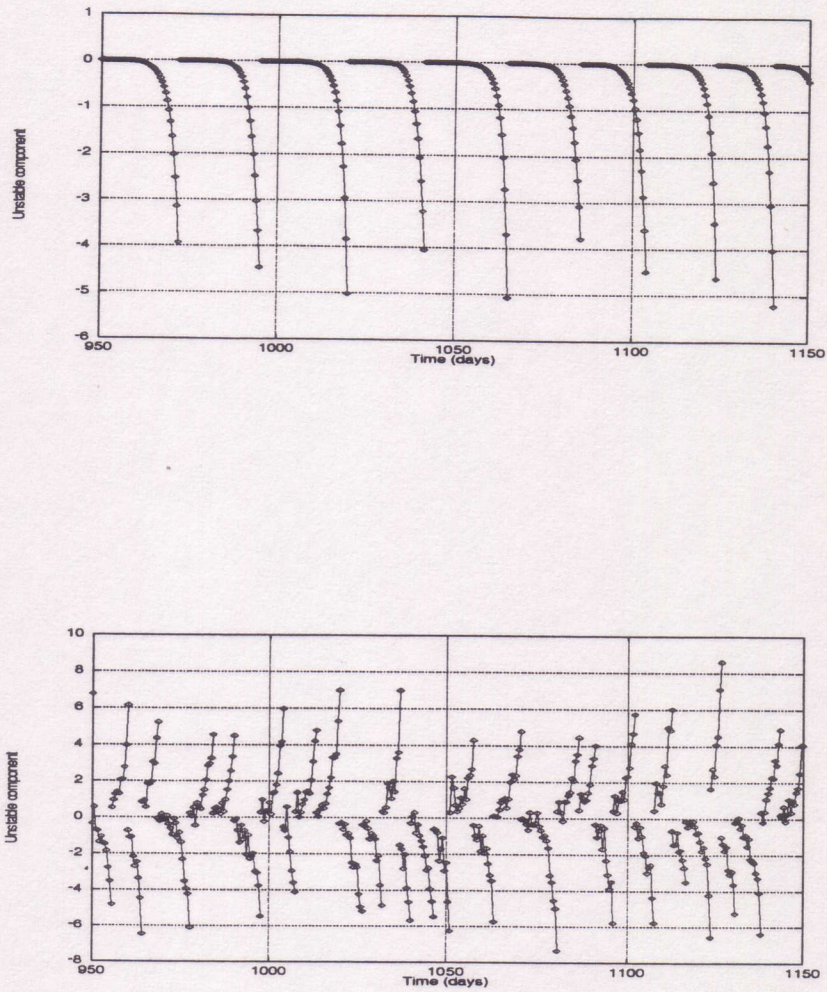


Figure 4 Evolution with time of the unstable component (in suitable units for the representation) of the controlled orbit. The dotted points correspond to the epochs at which the tracking has been performed. In the upper figure tracking and the maneuvers are performed without error. In the lower figure, errors in both parameters have been introduced. It is clearly seen, in this last situation, that the unstable component is not so nicely canceled as in the first one.

ACKNOWLEDGEMENTS

Portions of this work have been supported by Purdue University. The authors thank Brian Barden from Purdue University for assistance in implementation of the Target Point algorithm.

REFERENCES

1. R.W. Farquhar, "The Control and Use of Libration Point Satellites," NASA TR R-346, September 1970.
2. J.V. Breakwell, A.A. Kamel, and M.J. Ratner, "Station-Keeping for a Translunar Communications Station," *Celestial Mechanics*, Vol. 10, No. 3, 1974, pp. 357-373.
3. R.W. Farquhar, D.P. Muhonen, C.R. Newman, and H.S. Heuberger, "Trajectories and Orbital Maneuvers for the First Libration-Point Satellite," *Journal of Guidance and Control*, Vol. 3, No. 6, 1980, pp. 549-554.
4. K.C. Howell and H.J. Pernicka, "Stationkeeping Method for Libration Point Trajectories," *Journal of Guidance, Control, and Dynamics*, Vol. 16, No.1, January-February 1993, pp. 151-159.
5. K.C. Howell and S.C. Gordon, "Orbit Determination Error Analysis and a Station-Keeping Strategy for Sun-Earth L_1 Libration Point Orbits," *Journal of the Astronautical Sciences*, Vol. 42, No. 2, April-June 1994, pp. 207-228.
6. T.M. Keeter, "Station-Keeping Strategies for Libration Point Orbits: Target Point and Floquet Mode Approaches," M.S. Thesis, School of Aeronautics and Astronautics, Purdue University, West Lafayette, Indiana, 1994.
7. C. Simó, G. Gómez, J. Llibre, and R. Martínez, "Station Keeping of a Quasiperiodic Halo Orbit Using Invariant Manifolds," *Proceedings of the Second International Symposium on Spacecraft Flight Dynamics*, Darmstadt, Germany, October 1986, pp. 65-70.
8. C. Simó, G. Gómez, J. Llibre, R. Martínez, and R. Rodríguez, "On the Optimal Station Keeping Control of Halo Orbits," *Acta Astronautica*, Vol. 15, No.6/7, 1987, pp. 391-397.
9. G. Gómez, J. Masdemont, and C. Simó, "Quasihalo orbits associated with Libration Points," Preprint 1998.
10. M.A. Andreu and C. Simó, "Translunar Halo Orbits in the Quasibicircular Model," *Proceedings: The Dynamics of Small Bodies in the Solar System*, NATO ASI, Maratea, Italy, 1998 (to appear).
11. G. Gómez, A. Jorba, J. Masdemont, C. Simó, "Study of the Transfer from the Earth to a Halo Orbit Around the Equilibrium Point L_1 ," *Celestial Mechanics*, Vol. 56, 1993, pp. 541-562.
12. G. Gómez, A. Jorba, J. Masdemont, and C. Simó, "Study of the Transfer Between Halo Orbit," Preprint 1997.
13. W. Wiesel and W. Shelton, "Modal Control of an Unstable Periodic Orbit," *Journal of the Astronautical Sciences*, Vol. 31, 1983, pp. 63-76.